Cardiovascular Research (2016) **110**, 188–199
doi:10.1093/cvr/cvw047

Carfilzomib reverses pulmonary arterial hypertension

Xinhong Wang[1,2], Yasmine F. Ibrahim[1,3], Dividutta Das[1], Makhosazane Zungu-Edmondson[1], Nataliia V. Shults[1], and Yuichiro J. Suzuki[1]*

[1]Department of Pharmacology and Physiology, Georgetown University Medical Center, 3900 Reservoir Road NW, Washington, DC 20057, USA; [2]Department of Physiology and Pathophysiology, School of Basic Medical Sciences, Fudan University, Shanghai 200032, China; and [3]Department of Pharmacology, Minia University School of Medicine, Minia 61111, Egypt

Received 28 December 2015; revised 2 February 2016; accepted 19 February 2016; online publish-ahead-of-print 6 March 2016

Time for primary review: 29 days

Aims Pulmonary arterial hypertension (PAH) remains a lethal disease with pronounced narrowing of pulmonary vessels due to abnormal cell growth. Agents that can reduce the pulmonary vascular thickness thus have therapeutic potential. The present study investigated the efficacy of carfilzomib (CFZ), a proteasome inhibitor and a cancer chemotherapeutic drug, on reversing PAH.

Methods and results In two rat models of PAH, SU5416/hypoxia and SU5416/ovalbumin, CFZ effectively reversed pulmonary vascular remodelling with the promotion of apoptosis and autophagy. In human pulmonary artery smooth muscle cells, knocking down mediators of autophagy attenuated CFZ-induced cell death. The cell death role of autophagy was promoted by the participation of tumour protein p53-inducible nuclear protein 1. CFZ increased the protein ubiquitination, and siRNA knockdown of ubiquitin inhibited cell death, suggesting that CFZ-induced cell death is ubiquitin-dependent. Mass spectrometry demonstrated the ubiquitination of major vault protein and heat shock protein 90 in response to CFZ. The siRNA knockdown of these proteins enhanced CFZ-induced cell death, revealing that they are cell survival factors. CFZ reduced right-ventricular pressure and enhanced the efficacy of a vasodilator, sodium nitroprusside. While no indications of CFZ toxicity were observed in the right ventricle of PAH rats, apoptosis was promoted in the left ventricle. Apoptosis was prevented by dexrazoxane or by pifithrin-α without interfering with the efficacy of CFZ to reverse pulmonary vascular remodelling.

Conclusion The addition of anti-tumour agents such as CFZ along with cardioprotectants to currently available vasodilators may be a promising way to improve PAH therapy.

Keywords Apoptosis • Carfilzomib • Proteasome inhibitor • Pulmonary heart disease • Pulmonary hypertension

1. Introduction

Pulmonary arterial hypertension (PAH) is characterized by increased blood pressure in the pulmonary circulation and the development of pulmonary vascular remodelling.[1–3] Increased resistance in the pulmonary vessels strains the right ventricle (RV), leading to right heart failure. If untreated, the median survival of PAH patients after diagnosis has been reported to be 2.8 years with 3-year survival being 48%.[4] More recent studies have shown that, even with the currently available therapeutic agents, the 3-year survival of PAH patients is only 58–75%.[5–7] Thus, improved therapeutic strategies are needed to more satisfactorily treat PAH patients.

Although pulmonary vascular remodelling is a major factor in contributing to increased pulmonary vascular resistance, the actions of currently available drugs are largely limited to promoting vasodilation rather than reversing vascular remodelling.[8] Thus, agents that can reverse pulmonary vascular remodelling by eliminating excess pulmonary vascular cells should have therapeutic potential.[9,10]

Proteasome inhibitors are promising therapeutic agents for the treatment of cancer.[11] Bortezomib (BTZ) was the first proteasome inhibitor to be approved by the FDA, initially obtained approval for the treatment of refractory multiple myeloma in 2003.[12] In 2008, FDA approved BTZ for the initial treatment of patients with multiple myeloma. BTZ reversibly inhibits the chymotrypsin-like activity of the proteasome and promotes apoptosis of cancer cells. Some patients, however, do not respond to BTZ or only respond briefly and relapse. More recently in 2012, a second-generation proteasome inhibitor, carfilzomib (CFZ), was approved by the FDA for patients with multiple

* Corresponding author. Tel: +1 202 687 8090; fax: +1 202 687 8825, E-mail: ys82@georgetown.edu

myeloma who have received at least two prior therapies including BTZ, and it is considered to be a safe and effective alternative to BTZ.[13] CFZ is a tetrapeptide epoxy ketone analogue of epoxomicin that more selectively and irreversibly inhibits the chymotrypsin-like activity of the 20S proteasome, while BTZ is a reversible proteasome inhibitor.[14,15]

Since proteasome inhibition has been shown to suppress the growth of pulmonary artery smooth muscle cells (PASMCs),[16] proteasome inhibitors may be useful for treating PAH. Recent studies have shown that BTZ successfully reversed pulmonary vascular remodelling in rats.[10,17] However, the observations that BTZ caused cardiac apoptosis in both the RV and the left ventricle (LV) specifically in animals with PAH[17] may limit the clinical use of BTZ.

The present study evaluated the efficacy of CFZ on pulmonary vascular remodelling and PAH to determine if this proteasome inhibitor may be a safe and effective alternative to BTZ in the treatment of PAH.

2. Methods

2.1 Animal treatment

For the SU5416/hypoxia model,[18,19] male Sprague–Dawley rats were subcutaneously injected with SU5416 (20 mg/kg body weight), and then maintained in a hypoxia chamber regulated by an OxyCycler Oxygen Profile Controller (Model A84XOV; BioSpherix, Redfield, NY, USA) that was set to maintain 10% O_2 for 3 weeks, then in normoxia for 5 weeks. After pulmonary hypertension and pulmonary vascular remodelling were developed, animals were injected intraperitoneally with CFZ (Selleck Chemicals, Houston, TX, USA; 6 mg/kg body weight, twice a week for 2 weeks) as described in *Figure 1A*.

The SU5416/ovalbumin model was generated by administering ovalbumin and SU5416 as described by Mizuno *et al.*[20] After pulmonary hypertension and pulmonary vascular remodelling were developed, animals were injected with CFZ as described in Supplementary material online, *Figure S6A*.

At the end of the experiments, rats were anaesthetized with intraperitoneal injections of urethane (1.6 g/kg body weight). They were then intubated and mechanically ventilated with a volume-controlled Inspira Advanced Safety Ventilator (Harvard Apparatus, Holliston, MA, USA). Rats were maintained on a heat pad and the temperature was maintained at 37°C with a TR-200 Temperature Controller connected to a rectal probe (Fine Scientific Tools, North Vancouver, Canada). After a thoracotomy through the third left intercostal space, a Millar catheter (1.4 F) was inserted into the RV, and RV pressure was recorded by using PowerLab with Chart 5 software (AD Instruments, Colorado Springs, CO, USA).

The Georgetown University Animal Care and Use Committee approved all animal experiments (Protocol #13-044), and the investigation conformed to the National Institutes of Health Guide for the Care and Use of Laboratory Animals.

2.2 Histological measurements

Tissues were immersed in buffered 10% paraformaldehyde at room temperature and were embedded in paraffin. Paraffin-embedded tissues were cut and mounted on glass slides. Tissue sections were subjected to haematoxylin and eosin (H&E) stain, Verhoeff-van Gieson stain, Masson's trichrome stain, and immunohistochemistry with the α-smooth muscle actin antibody (Abcam, Cambridge, MA, USA). Slides were blinded and analysed microscopically for pulmonary arterial wall thicknesses and vessel diameters. Eight to 10 vessels were analysed per animal, and six values for the thickness and two values for the diameter were measured for each vessel. Percentage wall thickness (wall thickness divided by vessel diameter) was calculated by using IP Lab Software (Scanalytics Inc., VA, USA). Tissue sections were also evaluated for the occurrence of apoptosis by terminal deoxynucleotidyl transferase dUTP nick end labelling (TUNEL) assay using the ApopTag Peroxidase in Situ Apoptosis Detection Kit (Millipore, Billerica, MA, USA). % TUNEL positive-cells were calculated by assessing the number of apoptotic cells (brown stain) and the number of total cell nuclei (blue stain).

2.3 Western blot analysis

Extrapulmonary arteries (left and right main branches) and intrapulmonary arteries (first-order branch) were surgically dissected, and connective tissues were gently removed in ice-cold PBS under a dissecting microscope. Tissues were minced and homogenized, and protein gel electrophoresis samples were prepared.[10] For western blotting, equal protein amounts of samples or immunoprecipitates were electrophoresed through a reducing SDS polyacrylamide gel and electroblotted onto a membrane. The membrane was blocked and incubated with antibodies against cleaved caspase-3, LC3B, phosphorylated adenosine monophosphate-activated protein kinase (AMPK), p53-inducible nuclear protein 1 (TP53INP1), ubiquitin (Cell Signaling Technology, Danvers, MA, USA), Bcl-x_L, heat shock protein 90 (HSP90), major vault protein (MVP), AMPK (Santa Cruz Biotechnology, Dallas, TX, USA), and p62 (Syd Labs, Inc., Malden, MA, USA). Levels of proteins were detected using horseradish peroxidase-linked secondary antibodies and an Enhanced Chemiluminescence System (GE Healthcare Bio-Sciences, Pittsburgh, PA, USA).

2.4 Cell culture experiments

Human PASMCs (HPASMCs; ScienCell Research Laboratories, Carlsbad, CA, USA) were cultured in accordance with the manufacturer's instructions in 5% CO_2 at 37°C. Cells from four donors in passages 3–7 were used. CFZ was dissolved in DMSO and equal amounts of DMSO were added to controls. For siRNA knockdown, cells were transfected with gene silencing siRNAs or with the control siRNA containing a scrambled sequence using the siRNA Transfection Reagent (Santa Cruz). Cells were used for experiments 2 days after transfection. Cell number was determined using Cell Counting Kit-8 (Dojindo Molecular Technologies, Inc., Rockville, MD, USA) or by counting on a haemocytometer.

2.5 Statistical analysis

Means and standard errors were calculated. Comparisons between two groups were analysed by using a two-tailed Student's *t* test, while comparisons between three or more groups were analysed by using two-way analysis of variance (ANOVA) with a Student–Newman–Keuls *post-hoc* test in accordance with the Kolmogorov–Smirnov test for normality. Comparisons between three or more groups in dose or time response experiments in cultured cells were analysed by one-way ANOVA followed with Tukey's multiple comparison tests. $P < 0.05$ was considered to be significant.

3. Results

3.1 CFZ is more effective in killing human pulmonary vascular cells than BTZ

Cultured human pulmonary artery smooth muscle cells (HPASMCs) were treated with various doses of BTZ and CFZ and their abilities to kill pulmonary vascular cells were determined by a cell viability assay. We observed dose-dependent decreases in the cell number by both drugs (see Supplementary material online, *Figure S1*). CFZ was found to be more effective than BTZ, suggesting that CFZ may be useful for treating PAH. These results became a basis for testing the effects of CFZ in intact animals in the present study.

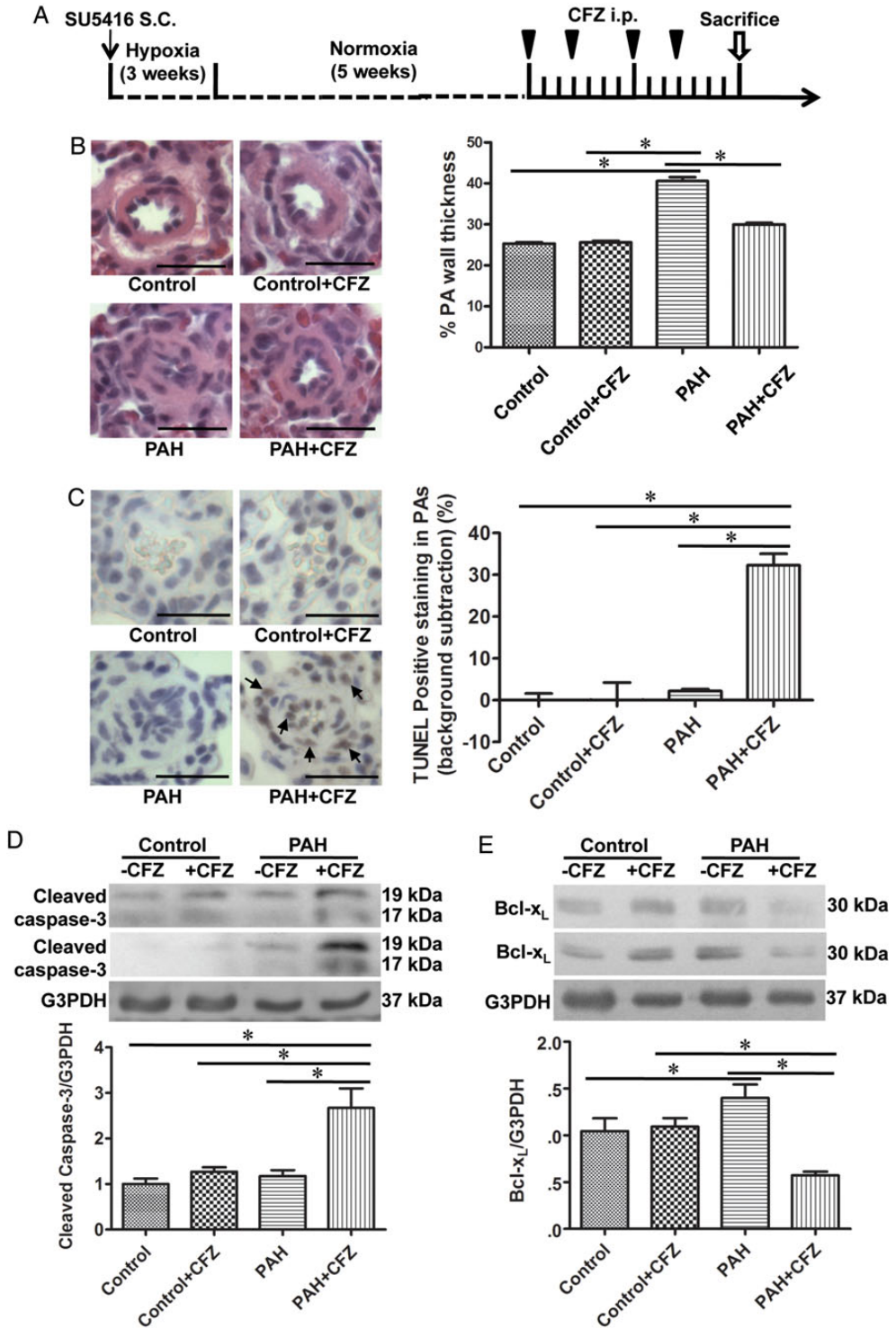

Figure 1 CFZ reduces the wall thickness of remodelled pulmonary arteries (PAs) and promotes apoptosis without affecting normal PAs in SU5416/hypoxia model of PAH. (*A*) Schematics of CFZ treatment in a rat model of PAH induced by SU5416 and hypoxia. Rats were injected with SU5416 and exposed to hypoxia for 3 weeks, and then placed in normoxia for 5 weeks. Rats were then injected with 6 mg/kg body weight CFZ, twice per week for 2 weeks. The rats were sacrificed after 3 days of the last injection. (*B*) Representative H&E staining of small PAs (diameters ranging from 50 to 100 μm). Scale bars, 50 μm. Bar graphs represent means ± SEM of percent wall thickness. (*C*) Representative TUNEL assay results. Scale bars, 50 μm. The bar graph represents means ± SEM of percent TUNEL positive cells in the small PAs after subtracting the background staining that were found in control lungs. (*D* and *E*) PAs were surgically isolated from rats, homogenized, and subjected to western blotting for cleaved caspase-3 and Bcl-x_L. Bar graphs represent means ± SEM. *Values significantly different from each other at $P < 0.05$. (Control, $n = 6$; Control + CFZ, $n = 6$; PAH, $n = 5$; PAH + CFZ, $n = 6$).

3.2 CFZ reverses pulmonary vascular remodelling and promotes apoptosis in HPASMCs

A combination of the injection of SU5416 (an inhibitor of VEGF receptor) and exposure to chronic hypoxia produces PAH that resembles human pathology in rats.[18,19] By using this model of PAH, effects of CFZ were examined. Rats were injected with SU5416 (20 mg/kg body weight) and subjected to chronic sustained hypoxia for 3 weeks. Subsequently, after being maintained in normoxia for 5 weeks, animals were injected with CFZ (6 mg/kg body weight) or the vehicle via the protocol that is described in *Figure 1A*. This treatment caused the development of severe pulmonary hypertension (systolic RV pressure of 63.0 $\pm$ 3.5 mmHg) and pulmonary vascular remodelling. H&E stain shows that the thickness of small pulmonary arteries was increased in response to the SU5416/hypoxia treatment and that CFZ significantly reversed this vascular thickening (*Figure 1B*). The enhanced intensity of α-smooth muscle actin stain and thickened smooth muscle walls were observed by immunohistochemistry in the pulmonary arterial wall media of PAH animals (see Supplementary material online, *Figure S2*; black arrow). This was partly reversed by CFZ, but slight intensely stained regions remained (see Supplementary material online, *Figure S2*; blue arrow). Verhoeff-van Gieson and Masson's trichrome stains show that pulmonary arteries of PAH animals have increased elastic fibres (see Supplementary material online, *Figure S3*; black arrows) and collagen fibres (see Supplementary material online, *Figures S3* and *S4*). The corrugation (blue arrow) and destruction of internal elastic lamina were also observed (see Supplementary material online, *Figure S3*). We also noted that 45–50% of pulmonary vessels contained collagen fibres within the medial layer (see Supplementary material online, *Figure S4*; arrows). These vascular remodelling events associated with PAH were reversed by CFZ (see Supplementary material online, *Figures S3* and *S4*).

The reversal of vascular remodelling was associated with the promotion of apoptosis as indicated by TUNEL staining (*Figure 1C*), cleaved caspase-3 (*Figure 1D*), and the down-regulation of the anti-apoptotic protein Bcl-x_L (*Figure 1E*). PAH was associated with increased TUNEL-positive cells in the alveoli and bronchial walls, but CFZ-treatment reduced apoptosis of non-pulmonary vessel regions of the lung (see Supplementary material online, *Figure S5*).

To confirm the effectiveness of CFZ in the reversal of pulmonary vascular remodelling, we used a newly developed model of PAH, which utilizes a combination of SU5416 injection and ovalbumin nebulization.[20] In this model, severe pulmonary hypertension (systolic RV pressure of 65.1 $\pm$ 4.5 mmHg) and pulmonary vascular remodelling were also observed. After the development of pulmonary vascular remodelling, rats were injected with CFZ (6 mg/kg body weight, i.p.) using the protocol described in Supplementary material online, *Figure S6A*. We found that the CFZ administration reversed pulmonary vascular remodelling (see Supplementary material online, *Figure S6B*), promoted apoptosis as indicated by TUNEL assays (see Supplementary material online, *Figure S6C*), cleaved caspase-3 (see Supplementary material online, *Figure S6D*), and down-regulated Bcl-x_L (see Supplementary material online, *Figure S6E*).

In cultured HPASMCs, CFZ was found to promote cell death (see Supplementary material online, *Figure S7A*), cleave caspase-3, and down-regulate Bcl-x_L expression in a dose- (see Supplementary material online, *Figure S7B*) and time- (see Supplementary material online, *Figure S7C*) dependent fashion.

3.3 CFZ promotes autophagic cell death

Indications of the occurrence of autophagy were also obtained by monitoring increased LC3B-II (*Figure 2A*) and the down-regulation of p62 (*Figure 2B*) in the SU5416/hypoxia model of PAH in rats. In cultured HPASMCs, CFZ promoted autophagy in a dose- (see Supplementary material online, *Figure S8A*) and time- (see Supplementary material online, *Figure S8B*) dependent fashion. An early signalling event that triggers autophagy, the phosphorylation of AMP kinase, was also activated by CFZ (see Supplementary material online, *Figure S8C*).

Since autophagy can trigger both cell death and cell survival,[21] siRNA was used to knockdown the mediators of autophagy to clarify the role of autophagy in CFZ actions. The siRNA knockdown of LC3B (*Figure 2C*) and AMPK (*Figure 2D*) in HPASMCs inhibited CFZ-induced cell death, indicating that autophagy mediates cell death.

Seillier *et al.*[22] described the role of tumour protein p53-inducible nuclear protein 1 (TP53INP1) in turning autophagy into a cell-death mechanism by interacting with LC3B-II. Consistently, the siRNA knockdown of TP53INP1 inhibited CFZ-induced cell death (*Figure 2E*) and CFZ promoted interactions between TP53INP1 and LC3B-II (*Figure 2F*).

3.4 CFZ-mediated cell death is ubiquitination-dependent

To test the hypothesis that cell killing by this proteasome inhibitor may be through the accumulation of ubiquitinated proteins, we tested the effects of CFZ on protein ubiquitination. The increased ubiquitination of various proteins was observed in the homogenates of isolated pulmonary arteries from normal or PAH rats treated with CFZ in SU5416/hypoxia (*Figure 3A*) and in SU5416/ovalbumin (*Figure 3B*) models. In HPASMCs, amounts of various ubiquitinated proteins were increased in response to the CFZ treatment of HPASMCs in a dose- (*Figure 3C*) and time- (*Figure 3D*) dependent fashion. To assess the functions of ubiquitin in CFZ-induced cell death, ubiquitin was knocked down by siRNA (*Figure 4A*). The siRNA knockdown of ubiquitin in HPASMCs significantly inhibited CFZ-induced cell death (*Figure 4B*), p62 down-regulation (*Figure 4C*), and Bcl-x_L down-regulation (*Figure 4D*), indicating that protein ubiquitination mediates CFZ-induced cell death. Further, siRNA knockdown of ubiquitin inhibited CFZ-mediated interactions between TP53INP1 and LC3B-II (*Figure 4E*). Thus, ubiquitinated proteins likely promote TP53INP1/LC3B-II interactions, which result in autophagy to mediate cell death.

To identify proteins whose ubiquitination is increased in response to the CFZ treatment, HPASMC lysates were immunoprecipitated with an ubiquitin antibody, and bands were visualized with Coomassie Blue staining. Two bands that contain proteins whose ubiquitination were consistently increased by the CFZ treatment of HPASMCs (*Figure 5A*) were excised and analysed by mass spectrometry. Results showed that major vault protein (MVP) and heat shock protein 90 (HSP90) were found to be ubiquitinated by CFZ. The ubiquitination of MVP by CFZ in HPASMCs was confirmed by immunoprecipitation with the ubiquitin antibody, followed by immunoblotting with the MVP antibody (*Figure 5B*). In rats, the ubiquitination of MVP by CFZ was found to specifically occur in pulmonary arteries with vascular remodelling compared with normal controls in the SU5416/ovalbumin (*Figure 5C*) and SU5416/hypoxia (*Figure 5D*) models of PAH. Similarly, immunoprecipitation/immunoblotting confirmed the ubiquitination of

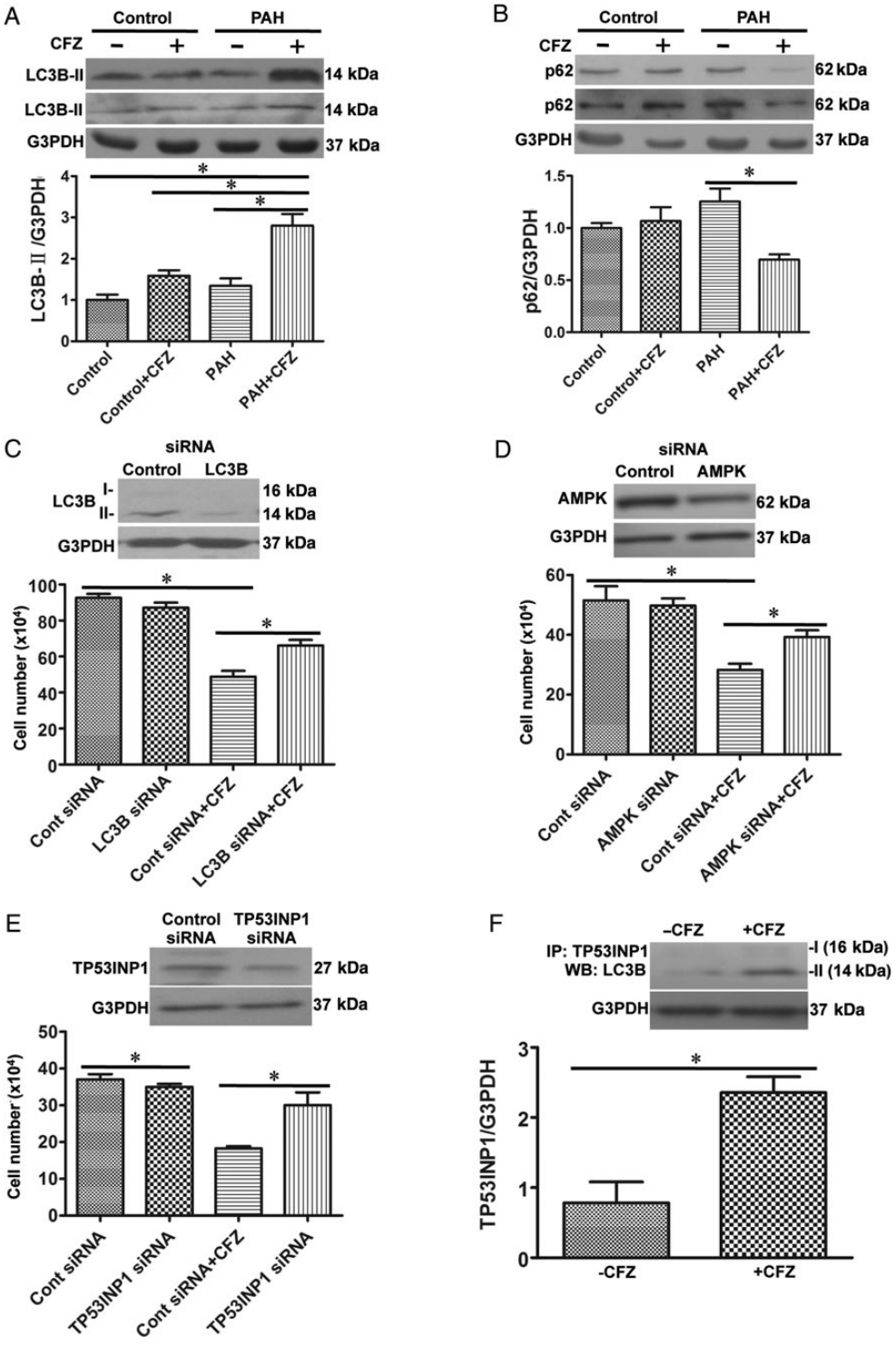

Figure 2 CFZ induces autophagic cell death. (*A* and *B*) Pulmonary arteries (PAs) were surgically isolated from rats subjected to SU5416/hypoxia treatment with remodelled PA and from normal rats, homogenized, and subjected to western blotting analysis for LC3B-II and p62 expression. Bar graphs represent means ± SEM. *Values significantly different from each other at $P < 0.05$. (Control, $n = 6$; Control + CFZ, $n = 6$; PAH, $n = 5$; PAH + CFZ, $n = 6$). (*C*–*E*) HPASMCs were transfected with control siRNA and LC3B, AMPK or TP53INP1 siRNA. After 48 h, transfection medium were changed to starvation medium for 4 h, and then HPASMCs were treated with CFZ (0.3 μM) for 20 h. Bar graphs show the cell number determined by counting on a haemocytometer (LC3B siRNA, $n = 6$; AMPK siRNA, $n = 4$; TP53INP1, $n = 4$). *Values significantly different from each other at $P < 0.05$. (*F*) HPASMCs were treated with CFZ (0.3 μM) for 20 h, and cell lysates were immunoprecipitated (IP) with TP53INP1 antibody, followed by immunoblotting with the LC3B antibody. The bar graph represents means ± SEM. *Values significantly different from each other at $P < 0.05 (n = 3)$.

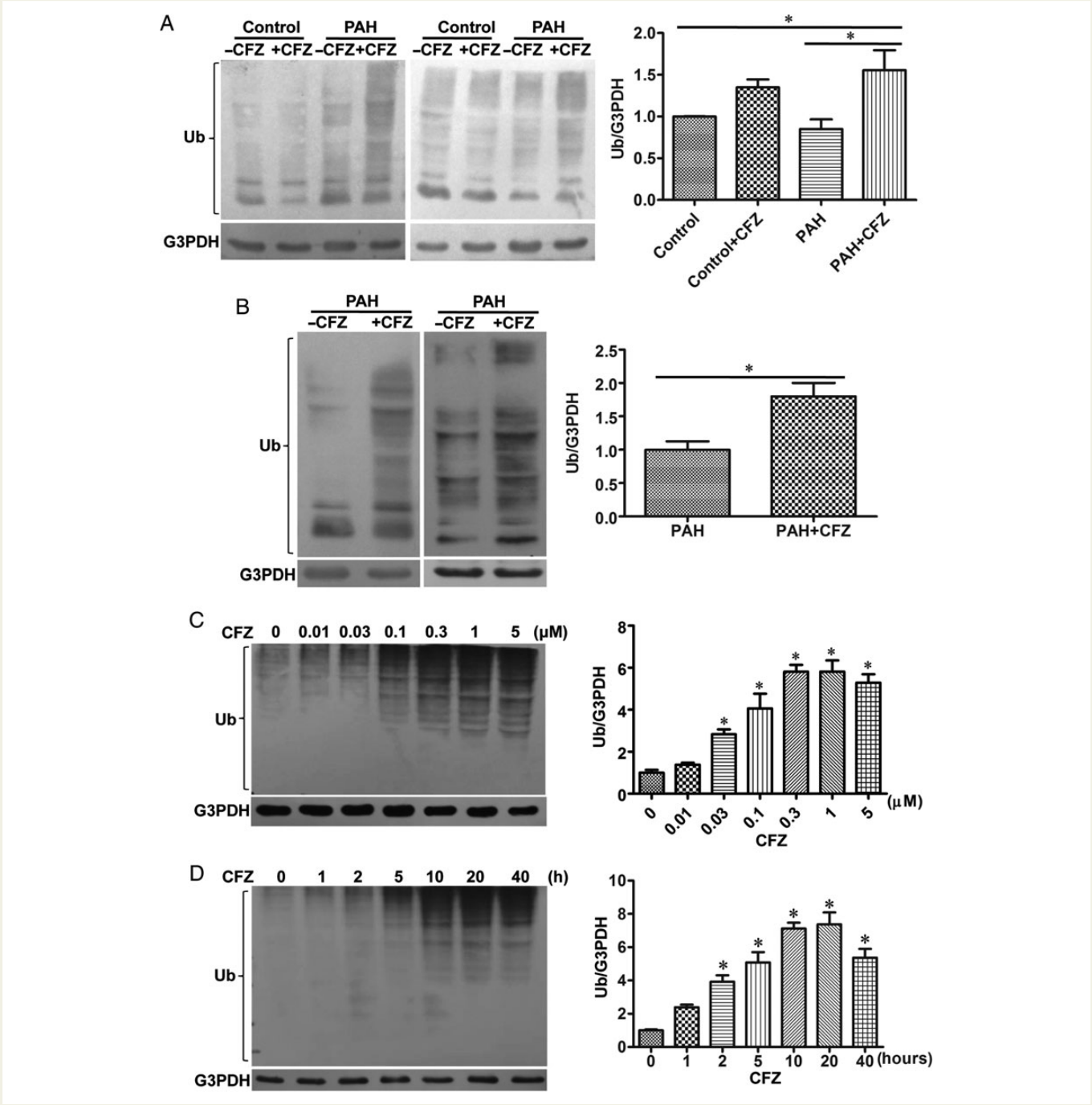

Figure 3 CFZ induces protein ubiquitination. (*A*) Isolated pulmonary arteries from the SU5416/hypoxia model of PAH were homogenized, and subjected to western blotting to monitor protein ubiquitination using a ubiquitin (Ub) antibody. (Control, $n = 6$; Control + CFZ, $n = 6$; PAH, $n = 5$; PAH + CFZ, $n = 6$). (*B*) Protein ubiquitination was monitored in isolated pulmonary arteries from the SU5416/ovalbumin model of PAH. (PAH, $n = 6$; PAH + CFZ, $n = 6$). Bar graphs represent means ± SEM. *Values significantly different from each other at $P < 0.05$. (*C*) HPASMCs were treated with various doses of CFZ for 20 h. Cell lysates were analysed for protein ubiquitination by western blotting. (*D*) Cells were treated with CFZ (0.3 μM) for various durations. Bar graphs represent means ± SEM. *Values significantly different from untreated control at $P < 0.05$ ($n = 6$).

HSP90 by CFZ (*Figure 5E–G*). CFZ did not increase MVP or HSP90 protein expression in any of these systems (see Supplementary material online, *Figure S9A–F*).

To determine the functions of MVP and HSP90 in HPASMCs, these proteins were knocked down by siRNA. The knockdown of either MVP (*Figure 5H*) or HSP90 (*Figure 5I*), as indicated by western blotting, significantly enhanced CFZ-induced cell death. Thus, these proteins may serve as cell survival factors, and the ubiquitination of these proteins in remodelled pulmonary vessels may mediate cell death.

3.5 CFZ enhances the actions of a vasodilator to reduce RV pressure

To determine if CFZ can decrease blood pressure in the pulmonary circulation, we monitored RV pressure by using a Millar

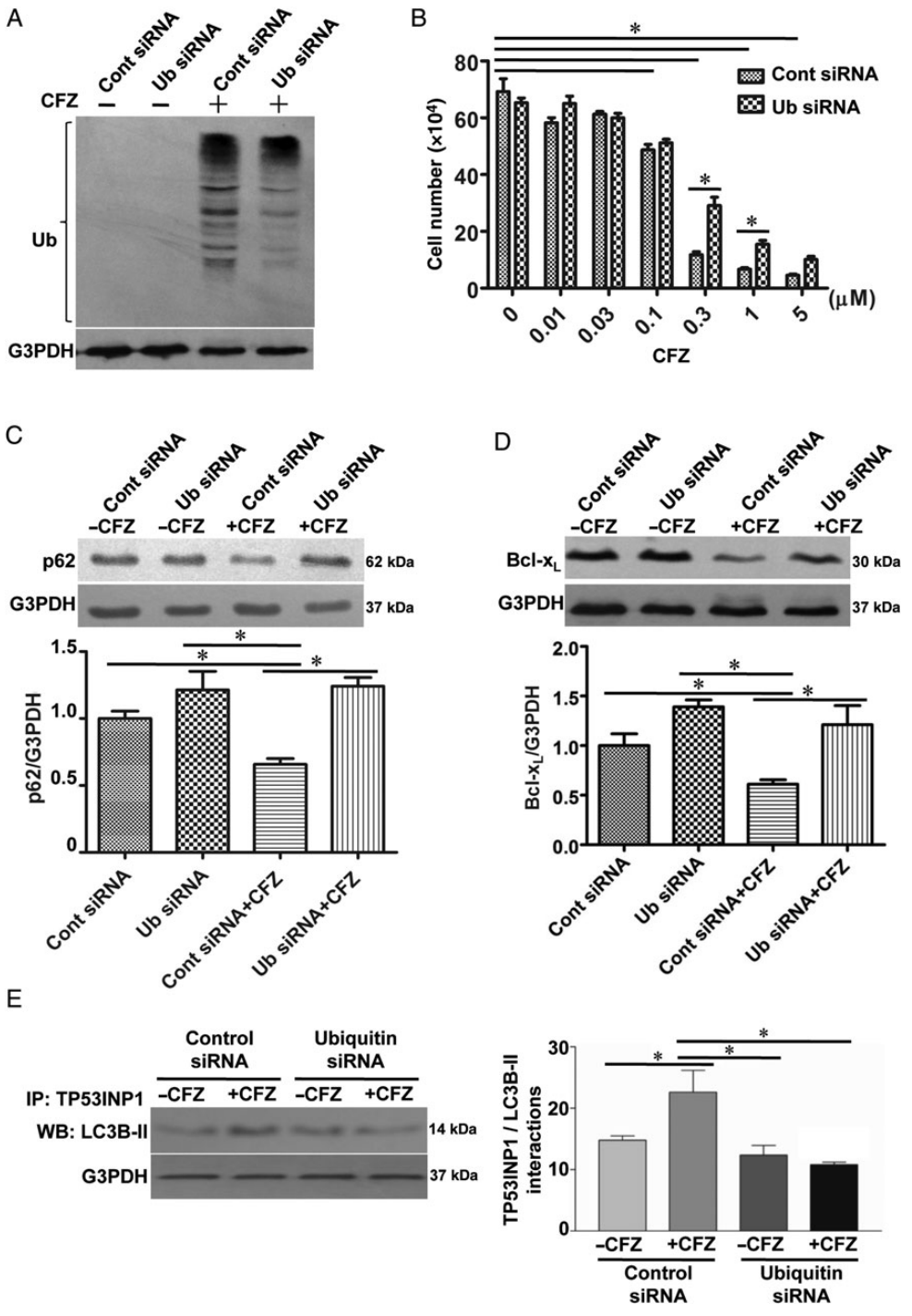

Figure 4 CFZ-induced cell killing is ubiquitin-dependent. HPASMCs were transfected with control siRNA and Ub siRNA. (*A*) Knocking down efficiency was monitored by western blotting. (*B*) After transfection for 48 h, the transfection medium was changed to the starvation medium. Four hours later, cells were treated with CFZ (0.3 μM) for 20 h. The cell number was determined by counting on a haemocytometer. (*C* and *D*) Cell lysates were subjected to immunoblotting to analyse the expression of p62 and Bcl-x_L. (*E*) Cell lysates were immunoprecipitated (IP) with TP53INP1 antibody, followed by immunoblotting with the LC3B antibody. The bar graphs represent means ± SEM. *Values significantly different from each other at $P < 0.05$ ($n = 4$).

catheter in anaesthetized, ventilated, open-chested rats. We found that CFZ treatment alone was sufficient to significantly reduce RV pressure (*Figure 6A* and *B*). Consistently, CFZ reduced RV hypertrophy as monitored by determining Fulton index (*Figure 6D*). Moreover, rats that received CFZ were significantly more susceptible to the reduction of RV pressure by a vasodilator, sodium nitroprusside (*Figure 6A* and *B*). CFZ had no effects on heart rate (*Figure 6C*).

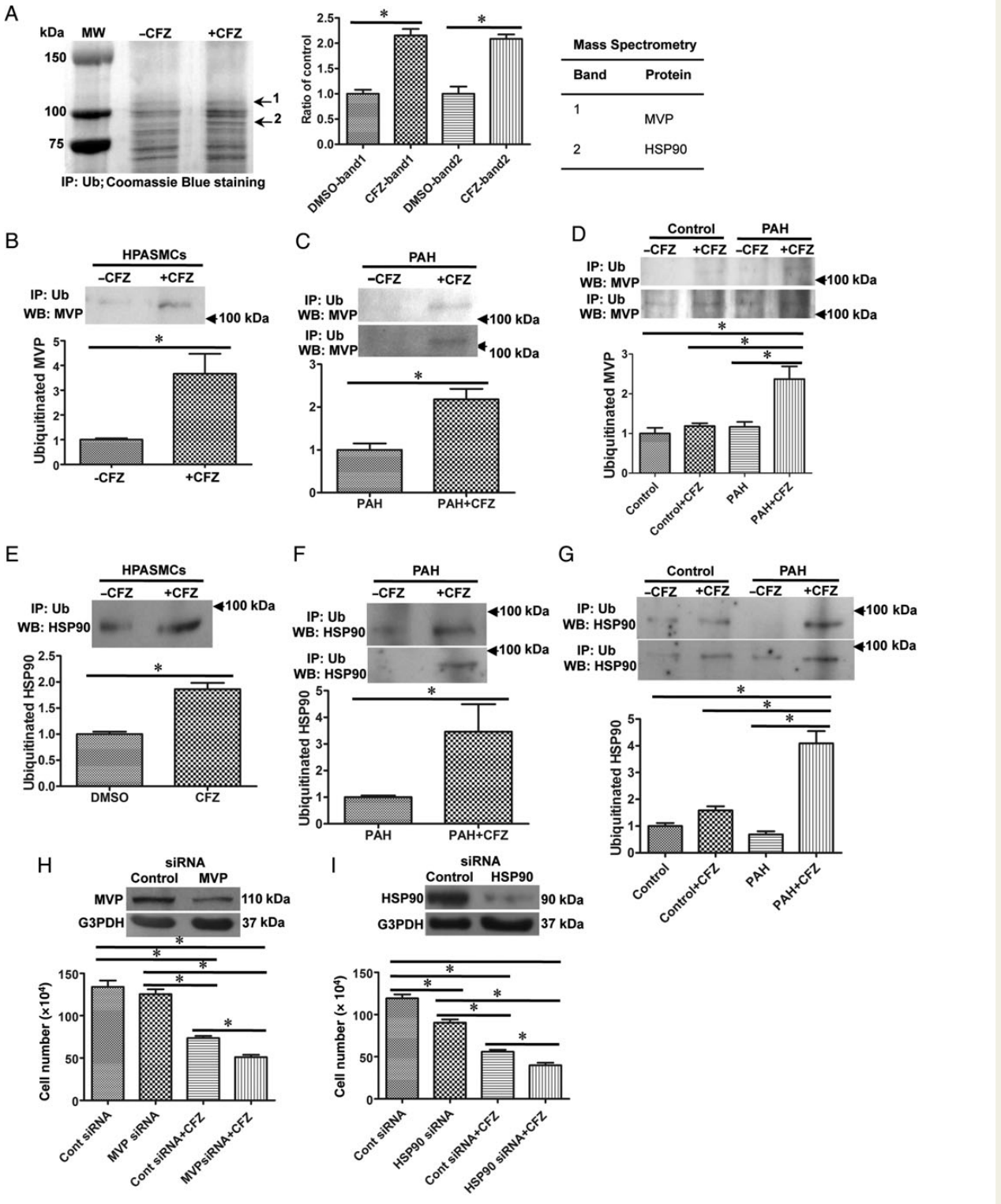

Figure 5 Identifications of proteins that are ubiquitinated by CFZ. (*A*) HPASMCs were treated with CFZ (0.3 μM) for 20 h, and cell lysates were immunoprecipitated (IP) with the Ub antibody. Bands indicated by arrows in Coomassie Blue-stained gels were consistently increased by CFZ treatment. The bar graph represents means ± SEM ($n = 3$). Mass spectrometry identified that these bands contain MVP and HSP90. Ubiquitination of MVP was confirmed in (*B*) CFZ-treated HPASMCs ($n = 6$), (*C*) isolated pulmonary arteries from SU5416/ovalbumin model ($n = 4$), and (*D*) isolated pulmonary arteries from SU5416/hypoxia model ($n = 4$) by immunoprecipitation with Ub antibody followed by immunoblotting with MVP. The ubiquitination of HSP90 were confirmed in (*E*) CFZ-treated HPASMCs ($n = 6$), (*F*) isolated pulmonary arteries from SU5416/ovalbumin model ($n = 6$), and (*G*) isolated pulmonary arteries from SU5416/hypoxia model ($n = 4$) by immunoprecipitation with Ub antibody followed by immunoblotting with HSP90 antibody. (*H* and *I*) HPASMCs were transfected with siRNA to knockdown MVP or HSP90. Efficiency of siRNA knockdown is shown in the western blotting data. Cells were treated with CFZ (0.3 μM) for 20 h, and the cell number was determined by counting on a haemocytometer. (MVP siRNA, $n = 5$; HSP90 siRNA, $n = 6$). *Values significantly different from each other at $P < 0.05$.

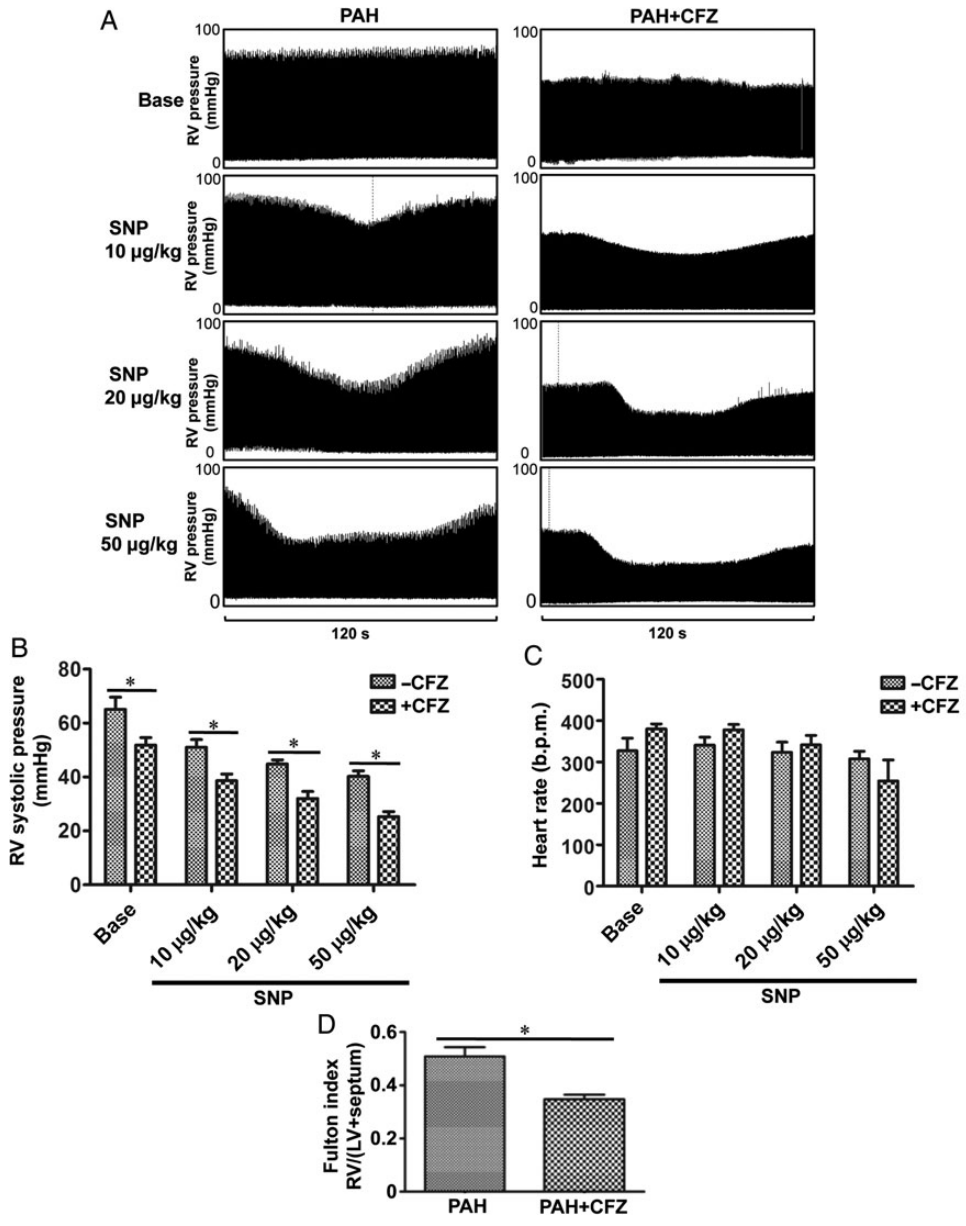

Figure 6 CFZ decreases RV pressure in PAH rats and increases the susceptibility of vasodilators to reduce RV pressure. PAH rats (SU5416/ovalbumin) were injected with CFZ (6 mg/kg body weight), twice a week. Three days after the last injection, rats were anaesthetized and mechanically ventilated. A Millar catheter was inserted into the RV apex to record RV pressure. After stabilization of haemodynamic recording for 10 min, sodium nitroprusside (SNP; 10, 20, or 50 μg/kg body weight) was slowly administered through the jugular vein in a 100 μL injection volume. (*A*) Representative homodynamic recording. (*B*) The bar graph represents means ± SEM of RV systolic pressure (DMSO, $n = 6$; CFZ, $n = 5$). (*C*) The bar graph represents means ± SEM of the heart rate. (*D*) The bar graph represents means ± SEM of Fulton index. *$P < 0.05$.

3.6 Effects of CFZ on the heart

We investigated whether CFZ exerts cardiotoxicity. No indications of CFZ toxicity to the hypertrophied RV were found; RV contractility as assessed by measuring d*P*/d*t* was unaltered (see Supplementary material online, *Figure S10A*). Further, measurements of cleaved caspase-3 (see Supplementary material online, *Figure S10B*) and anti-apoptotic Bcl-x_L expression (see Supplementary material online, *Figure S10C*) showed no indication of the occurrence of apoptosis in the hypertrophied RV in response to CFZ. These results suggest that the RVs of PAH animals are resistant to CFZ.

In contrast, a marked cleaved caspase-3 formation was noted in the LV of PAH animals treated with CFZ (*Figure 7A*). We tested whether myocardial apoptosis in the LV of rats with PAH can be suppressed by giving dexrazoxane, an FDA-approved cardioprotective agent used in cancer chemotherapy,[23,24] or pifithrin-α, an inhibitor of p53 thus an inhibitor of heart failure.[25] Rats treated with SU5416 and hypoxia to induce PAH were treated with a combination of CFZ and dexrazoxane (50 mg/kg) or pifithrin-α (2.2 mg/kg) injected intraperitoneally along with 6 mg/kg body weight CFZ, twice per week for 2 weeks. Results showed that the administration of dexrazoxane or pifithrin-α inhibited

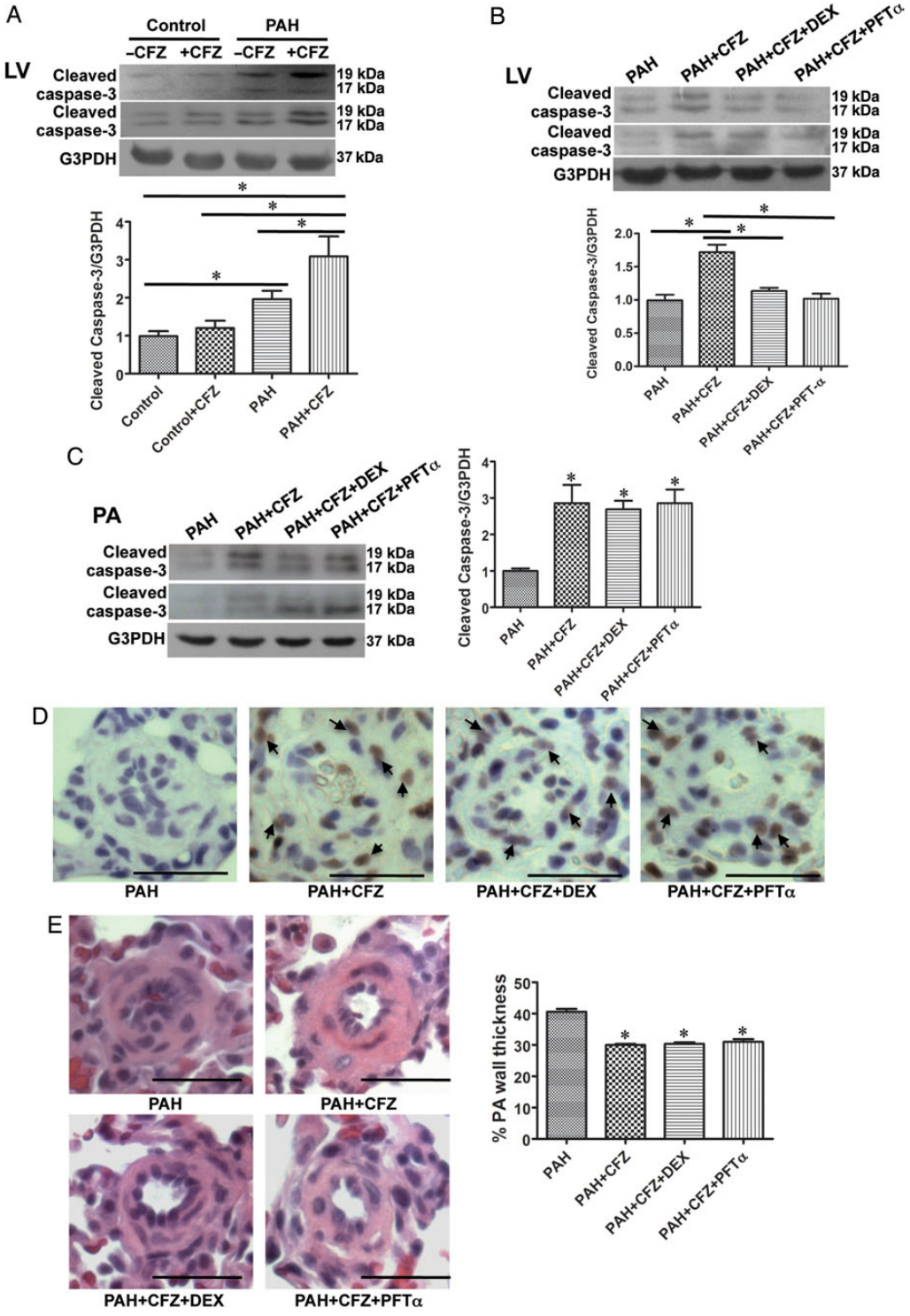

Figure 7 Dexrazoxane (DEX) and pifithrin-α (PFT-α) protects the left ventricle (LV) from CFZ-induced apoptosis without affecting the efficacy of CFZ in reversing PA remodelling. (*A*) In SU5416/hypoxia model of PAH, cleaved caspase-3 formation in the LV was analysed by western blotting. *Values significantly different from each other at $P < 0.05$. (Control, $n = 6$; Control + CFZ, $n = 6$; PAH, $n = 5$; PAH + CFZ, $n = 6$). (*B*) PAH rats (SU5416/hypoxia) were divided into four groups to determine the protective effects of DEX or PFTα. DEX (50 mg/kg) or PFT-α (2.2 mg/kg) was injected intraperitoneally along with 6 mg/kg body weight CFZ, twice a week for 2 weeks. Rats were then sacrificed 3 days after the last injection. LV tissues were homogenized, and subjected to western blotting for cleaved capase-3 formation. (*C*) Pulmonary arteries (PA) from these rats were surgically isolated, homogenized, and subjected to western blotting analysis for cleaved caspase-3. (*D*) Apoptosis in remodelled small PA induced by CFZ was not affected by DEX or PFT-α as shown in TUNEL staining. (*E*) The reduction of remodelled PA thickness induced by CFZ was not affected by DEX or PFT-α by analysing H&E staining. *Values in bar graphs denote significantly different from values from untreated PAH rats at $P < 0.05$. (PAH, $n = 5$; PAH + CFZ, $n = 6$; PAH + CFZ + DEX, $n = 5$; PAH + CFZ + PFT-α, $n = 6$).

CFZ-induced cardiotoxicity as monitored by assessing cleaved caspase-3 formation (*Figure 7B*).

Importantly, despite these agents being capable of inhibiting apoptosis induced by CFZ in the LV, neither cardioprotectants interfered with the ability of CFZ to promote apoptosis in pulmonary vessels (*Figure 7C* and *D*) or to reverse pulmonary vascular remodelling (*Figure 7E*).

4. Discussion

The major findings of this study are that (i) CFZ, a more recently approved proteasome inhibitor for the treatment of cancer,[13] effectively reversed pulmonary vascular remodelling and reduced RV pressure and (ii) cardiotoxicity exerted by CFZ can be eliminated by dexrazoxane or pifithrin-α.

Currently available treatment strategies for PAH are limited to the use of vasodilators. While these agents relieve some of the symptoms, their effects on patient survival are limited, possibly because the effects of currently available drugs on pulmonary vascular remodelling may be minimal. Thus, new therapeutic agents designed to specifically kill unwanted pulmonary vascular cells may be a promising avenue for more effectively managing this life-threatening disease. In this regard, the effectiveness of BTZ, the first proteasome inhibitor that was approved by the FDA for the treatment of cancer had been explored in experimental PAH.[10,17] While this drug showed promising effects in alleviating PAH, it also exhibited cardiotoxicity.[17] Since cardiotoxicity occurs in response to most, if not all anti-tumour drugs,[26] PAH treatment that may use these drugs needs to find ways to deal with this problem. The use of known cardiotoxic agents is more complicated for PAH treatment, as these patients have weakened hearts. One must decide if the benefit of reversing pulmonary vascular remodelling outweighs the risk of cardiac complications. This and previous studies[10] using experimental animal models have consistently shown that the RV affected by PAH is resistant to damage by various anti-tumour agents. Thus, the use of anti-tumour drugs in PAH patients may not necessarily be viewed as a contraindication.

In this study, however, we found that the LVs of PAH animals were affected by CFZ treatment. Specifically, apoptosis was promoted as monitored by the level of cleaved caspase-3. Remarkably, CFZ-induced apoptosis was inhibited by the administration of either dexrazoxane or pifithrin-α. Dexrazoxane is a cardioprotectant with iron chelating properties that has been approved by the FDA to be used in conjunction with anti-tumour drugs.[23,24] Pifithrin-α is an inhibitor of p53[27,28] that has been implicated in heart failure.[25] Importantly, neither of these drugs interfered with the ability to promote apoptosis in the pulmonary vasculature or to reverse pulmonary vascular remodelling. To our knowledge, this is the first demonstration of therapeutic strategies that allow for inhibiting cardiotoxicity without affecting the efficacy of primary drugs to alleviate PAH.

In addition to demonstrating the therapeutic efficacy of CFZ towards PAH and identifying possible cardioprotective agents that may be useful in PAH therapy, this study provided important mechanistic information. We showed that the CFZ-mediated death of PASMCs is dependent on apoptotic and autophagic cell death. AMPK is known to be an important upstream signalling molecule for entering autophagy or apoptosis.[29–31] Previous studies in HPASMCs showed that hypoxia activated AMPK and promoted cell survival.[32] In contrast, results from the present study demonstrated that AMPK is required for the CFZ-induced death of HPASMCs. These incompatible findings are consistent with observations by many laboratories that autophagy mediates both cell-survival and cell-death signals. Our results in the present study suggest that TP53INP1 specifically drives autophagy to cell death by interacting with LC3B-II in response to CFZ.

Further, while the induction of protein ubiquitination in response to proteasome inhibition was expected, we showed that ubiquitin knockdown inhibited CFZ-mediated apoptosis as well as autophagy. More specifically, ubiquitination appears to target the ability of TP53INP1 to bind to LC3B-II and interfere with the role of autophagy as a cell-survival mechanism. We were able to identify two of multiple ubiquitinated proteins in response to the CFZ treatment using mass spectrometry, namely MVP and HSP90. MVP, also known as lung resistance-related protein, is highly expressed in the lung.[33,34] MVP assembles the outer shell of the vault, which also contains vault poly (ADP-ribose)-polymerase, telomerase-associated protein, and untranslated vault RNA sequences.[34,35] Although MVP has been proposed to play a role in drug resistance, the biological functions of MVP have not been well defined. In this study, since knocking down MVP or HSP90 enhanced CFZ-mediated cell death, these proteins seem to serve as cell-survival factors in HPASMCs. Whether these proteins are mono-ubiquitinated or poly-ubiquitinated and the functions of ubiquitination of these two and other unidentified proteins in CFZ-induced cell death need further investigations.

This study presented novel information that may be clinically relevant and that advances the understanding of biological mechanisms centred on the potential use of CFZ, a recently approved anti-tumour drug, in the treatment of PAH. Our results suggest that CFZ in conjunction with vasodilators and cardioprotectants, perhaps dexrazoxane that is already approved to be used with anti-tumour drugs, may be an effective combination therapy for the treatment of PAH. We present novel mechanisms of proteasome inhibition, which involve the active role of ubiquitin in promoting apoptosis as well as autophagy that can lead to cell death via the action of TP53INP1. Our results may provide important and useful information for designing future experiments in order to find a cure for the deadly disease of PAH.

Supplementary material

Supplementary Material is available at *Cardiovascular Research* online.

Conflict of interest: none declared.

Funding

This work was supported in part by National Institutes of Health (R01HL72844) to Y.J.S.; and the National Natural Science Foundation of China (81201468) and Fudan University Fund (20520133217) to X.W. The content is solely the responsibility of the authors and does not necessarily represent the official views of the National Institutes of Health.

References

1. Archer SL, Michelakis ED. An evidence-based approach to the management of pulmonary arterial hypertension. *Curr Opin Cardiol* 2006;**21**:385–392.
2. Humbert M, Morrell NW, Archer SL, Stenmark KR, MacLean MR, Lang IM, Christman BW, Weir EK, Eickelberg O, Voelkel NF, Rabinovitch M. Cellular and molecular pathobiology of pulmonary arterial hypertension. *J Am Coll Cardiol* 2004;**43**:13S–24S.
3. Stacher E, Graham BB, Hunt JM, Gandjeva A, Groshong SD, McLaughlin VV, Jessup M, Grizzle WE, Aldred MA, Cool CD, Tuder RM. Modern age pathology of pulmonary arterial hypertension. *Am J Respir Crit Care Med* 2012;**186**:261–272.
4. D'Alonzo GE, Barst RJ, Ayres SM, Bergofsky EH, Brundage BH, Detre KM, Fishman AP, Goldring RM, Groves BM, Kernis JT, Levy PS, Pietra GG, Reid LM, Reeves JT, Rich S,

Vreim CE, Williams GW, Wu M. Survival in patients with primary pulmonary hypertension. Results from a national prospective registry. *Ann Intern Med* 1991;**115**:343–349.
5. Benza RL, Miller DP, Frost A, Barst RJ, Krichman AM, McGoon MD. Analysis of the lung allocation score estimation of risk of death in patients with pulmonary arterial hypertension using data from the REVEAL Registry. *Transplantation* 2010;**90**:298–305.
6. Humbert M, Sitbon O, Yaïci A, Montani D, O'Callaghan DS, Jaïs X, Parent F, Savale L, Natali D, Günther S, Chaouat A, Chabot F, Cordier JF, Habib G, Gressin V, Jing ZC, Souza R, Simonneau G, French Pulmonary Arterial Hypertension Network. Survival in incident and prevalent cohorts of patients with pulmonary arterial hypertension. *Eur Respir J* 2010;**36**:549–555.
7. Thenappan T, Shah SJ, Rich S, Tian L, Archer SL, Gomberg-Maitland M. Survival in pulmonary arterial hypertension: a reappraisal of the NIH risk stratification equation. *Eur Respir J* 2010;**35**:1079–1087.
8. Puri A, McGoon MD, Kushwaha SS. Pulmonary arterial hypertension: current therapeutic strategies. *Nat Clin Pract Cardiovasc Med* 2007;**4**:319–329.
9. Suzuki YJ, Nagase H, Wong CM, Kumar SV, Jain V, Park AM, Day RM. Regulation of Bcl-x_L expression in lung vascular smooth muscle. *Am J Respir Cell Mol Biol* 2007;**36**:678–687.
10. Ibrahim YF, Wong CM, Pavlickova L, Liu L, Trasar L, Bansal G, Suzuki YJ. Mechanism of the susceptibility of remodeled pulmonary vessels to drug-induced cell killing. *J Am Heart Assoc* 2014;**3**:e000520.
11. Giuliano M, D'Anneo A, De Blasio A, Vento R, Tesoriere G. Apoptosis meets proteasome, an invaluable therapeutic target of anticancer drugs. *Ital J Biochem* 2003;**52**:112–121.
12. Kane RC, Bross PF, Farrell AT, Pazdur R. Velcade: U.S. FDA approval for the treatment of multiple myeloma progressing on prior therapy. *Oncologist* 2003;**8**:508–513.
13. Herndon TM, Deisseroth A, Kaminskas E, Kane RC, Koti KM, Rothmann MD, Habtemariam B, Bullock J, Bray JD, Hawes J, Palmby TR, Jee J, Adams W, Mahayni H, Brown J, Dorantes A, Sridhara R, Farrell AT, Pazdur R. U.S. Food and Drug Administration approval: carfilzomib for the treatment of multiple myeloma. *Clin Cancer Res* 2013;**19**:4559–4563.
14. Demo SD, Kirk CJ, Aujay MA, Buchholz TJ, Dajee M, Ho MN, Jiang J, Laidig GJ, Lewis ER, Parlati F, Shenk KD, Smyth MS, Sun CM, Vallone MK, Woo TM, Molineaux CJ, Bennett MK. Antitumor activity of PR-171, a novel irreversible inhibitor of the proteasome. *Cancer Res* 2007;**67**:6383–6391.
15. Kortuem KM, Stewart AK. Carfilzomib. *Blood* 2013;**121**:893–897.
16. Li M, Dong X, Liu Y, Sun X, Li Z, He J. Inhibition of ubiquitin proteasome function suppresses proliferation of pulmonary artery smooth muscle cells. *Naunyn Schmiedebergs Arch Pharmacol* 2011;**384**:517–523.
17. Kim SY, Lee JH, Huh JW, Kim HJ, Park MK, Ro JY, Oh YM, Lee SD, Lee YS. Bortezomib alleviates experimental pulmonary arterial hypertension. *Am J Respir Cell Mol Biol* 2012;**47**:698–708.
18. Taraseviciene-Stewart L, Kasahara Y, Alger L, Hirth P, Mc Mahon G, Waltenberger J, Voelkel NF, Tuder RM. Inhibition of the VEGF receptor 2 combined with chronic hypoxia causes cell death-dependent pulmonary endothelial cell proliferation and severe pulmonary hypertension. *FASEB J* 2001;**15**:427–438.
19. Abe K, Toba M, Alzoubi A, Ito M, Fagan KA, Cool CD, Voelkel NF, McMurtry IF, Oka M. Formation of plexiform lesions in experimental severe pulmonary arterial hypertension. *Circulation* 2010;**121**:2747–2754.
20. Mizuno S, Farkas L, Al Husseini A, Farkas D, Gomez-Arroyo J, Kraskauskas D, Nicolls MR, Cool CD, Bogaard HJ, Voelkel NF. Severe pulmonary arterial hypertension induced by SU5416 and ovalbumin immunization. *Am J Respir Cell Mol Biol* 2012;**47**:679–687.
21. Levine B, Kroemer G. Autophagy in the pathogenesis of disease. *Cell* 2008;**132**:27–42.
22. Seillier M, Peuget S, Gayet O, Gauthier C, N'Guessan P, Monte M, Carrier A, Iovanna JL, Dusetti NJ. TP53INP1, a tumor suppressor, interacts with LC3 and ATG8-family proteins through the LC3-interacting region (LIR) and promotes autophagy-dependent cell death. *Cell Death Differ* 2012;**19**:1525–1535.
23. Herman EH, Zhang J, Rifai N, Lipshultz SE, Hasinoff BB, Chadwick DP, Knapton A, Chai J, Ferrans VJ. The use of serum levels of cardiac troponin T to compare the protective activity of dexrazoxane against doxorubicin- and mitoxantrone-induced cardiotoxicity. *Cancer Chemother Pharmacol* 2001;**48**:297–304.
24. Dickey JS, Gonzalez Y, Aryal B, Mog S, Nakamura AJ, Redon CE, Baxa U, Rosen E, Cheng G, Zielonka J, Parekh P, Mason KP, Joseph J, Kalyanaraman B, Bonner W, Herman E, Shacter E, Rao VA. Mito-tempol and dexrazoxane exhibit cardioprotective and chemotherapeutic effects through specific protein oxidation and autophagy in a syngeneic breast tumor preclinical model. *PLoS One* 2013;**8**:e70575.
25. Sano M, Minamino T, Toko H, Miyauchi H, Orimo M, Qin Y, Akazawa H, Tateno K, Kayama Y, Harada M, Shimizu I, Asahara T, Hamada H, Tomita S, Molkentin JD, Zou Y, Komuro I. p53-induced inhibition of Hif-1 causes cardiac dysfunction during pressure overload. *Nature* 2007;**446**:444–448.
26. Vincent DT, Ibrahim YF, Espey MG, Suzuki YJ. The role of antioxidants in the era of cardio-oncology. *Cancer Chemother Pharmacol* 2013;**72**:1157–1168.
27. Komarov PG, Komarova EA, Kondratov RV, Christov-Tselkov K, Coon JS, Chernov MV, Gudkov AV. A chemical inhibitor of p53 that protects mice from the side effects of cancer therapy. *Science* 1999;**285**:1733–1737.
28. Lorenzo E, Ruiz-Ruiz C, Quesada AJ, Hernández G, Rodríguez A, López-Rivas A, Redondo JM. Doxorubicin induces apoptosis and CD95 gene expression in human primary endothelial cells through a p53-dependent mechanism. *J Biol Chem* 2002;**277**:10883–10892.
29. Mishra R, Cool BL, Laderoute KR, Foretz M, Viollet B, Simonson MS. AMP-activated protein kinase inhibits transforming growth factor-beta-induced Smad3-dependent transcription and myofibroblast transdifferentiation. *J Biol Chem* 2008;**283**:10461–10469.
30. Igata M, Motoshima H, Tsuruzoe K, Kojima K, Matsumura T, Kondo T, Taguchi T, Nakamaru K, Yano M, Kukidome D, Matsumoto K, Toyonaga T, Asano T, Nishikawa T, Araki E. Adenosine monophosphate-activated protein kinase suppresses vascular smooth muscle cell proliferation through the inhibition of cell cycle progression. *Circ Res* 2005;**97**:837–844.
31. Nagata D, Takeda R, Sata M, Satonaka H, Suzuki E, Nagano T, Hirata Y. AMP-activated protein kinase inhibits angiotensin II–stimulated vascular smooth muscle cell proliferation. *Circulation* 2004;**110**:444–451.
32. Ibe JC, Zhou Q, Chen T, Tang H, Yuan JX, Raj JU, Zhou G. Adenosine monophosphate-activated protein kinase is required for pulmonary artery smooth muscle cell survival and the development of hypoxic pulmonary hypertension. *Am J Respir Cell Mol Biol* 2013;**49**:609–618.
33. Steiner E, Holzmann K, Elbling L, Micksche M, Berger W. Cellular functions of vaults and their involvement in multidrug resistance. *Curr Drug Targets* 2006;**7**:923–934.
34. Kowalski MP, Dubouix-Bourandy A, Bajmoczi M, Golan DE, Zaidi T, Coutinho-Sledge YS, Gygi MP, Gygi SP, Wiemer EA, Pier GB. Host resistance to lung infection mediated by major vault protein in epithelial cells. *Science* 2007;**317**:130–132.
35. Tanaka H, Kato K, Yamashita E, Sumizawa T, Zhou Y, Yao M, Iwasaki K, Yoshimura M, Tsukihara T. The structure of rat liver vault at 3.5 angstrom resolution. *Science* 2009;**323**:384–388.